View metadata, citation and similar papers at core.ac.uk
brought to you by CORE
provided by International Journal of Remote Sensing and Earth Sciences (IJReSES)

International Journal of Remote Sensing and Earth Sciences Vol. 16 No. 1 June 2019: 31–44

THE USE OF C-BAND SYNTHETIC APERTURE RADAR SATELLITE DATA FOR RICE PLANT GROWTH PHASE IDENTIFICATION

Anugrah Indah Lestari* and Dony Kushardono
Remote Sensing Application Center,
Indonesian National Institute of Aeronautics and Space
e-mail: anugrah.indah@lapan.go.id, dony_kushardono@lapan.go.id
Received: 30 July 2019 ; Revised: 10 September 2019 ; Approved: 11 September 2019

Abstract. Identification of the rice plant growth phase is an important step in estimating the harvest season and predicting rice production. It is undertaken to support the provision of information on national food availability. Indonesia's high cloud coverage throughout the year means it is not possible to make optimal use of optical remote sensing satellite systems. However, the Synthetic Aperture Radar (SAR) remote sensing satellite system is a promising alternative technology for identifying the rice plant growth phase since it is not influenced by cloud cover and the weather. This study uses multi-temporal C-Band SAR satellite data for the period May–September 2016. VH and VV polarisation were observed to identify the rice plant growth phase of the Ciherang variety, which is commonly planted by farmers in West Java. Development of the rice plant growth phase model was optimized by obtaining samples spatially from a rice paddy block in PT Sang Hyang Seri, Subang, in order to acquire representative radar backscatter values from the SAR data on the age of certain rice plants. The Normalised Difference Polarisation Index (NDPI) and texture features, namely entropy, homogeneity and the Grey-Level Co-occurrence Matrix (GLCM) mean, were included as the samples. The results show that the radar backscatter value (σ^0) of VH polarisation without the texture feature, with the entropy texture feature and GLCM mean texture feature respectively exhibit similar trends and demonstrate potential for use in identifying and monitoring the rice plant growth phase. The rice plant growth phase model without texture feature on VH polarisation is revealed as the most suitable model since it has the smallest average error.

Keywords: *remote sensing satellite; SAR; C-band; texture feature; rice plant growth phase*

1 INTRODUCTION

Rice is a staple food consumed by the Indonesian population in both urban and rural areas. In 2008, the per capita rice consumption was 100.52 kg/year (Mauludyani et al., 2008), with an average consumption during the period 2010–2014 of 9.5 kg/capita/year (Badan Pengkajian & Pengembangan Perdagangan, 2016). Indonesia's population is projected to rise from 238.5 million in 2010 to 305.6 million in 2035 (BPS, 2013), with a particular demographic boost during the period 2020–2030 (Noor, 2015). Therefore, a government strategy is required to help ensure national food security.

The formation of policy in areas such as rice importation typically requires rice production estimation data to be available quickly and to cover a large area. As such, remote sensing is one of the technologies that can be used to support national food security. The use of remote sensing can enable the rapid retrieval of geo-biophysics parameters that cover a large area. The rice plant growth phase determined using remote sensing data can be used to forecast the harvest season (Ferencz et al., 2004) in order to acquire estimation data on rice production.

The rice plant growth phase has been identified and monitored using the

http://dx.doi.org/10.30536/j.ijreses.2019.a3171
@Indonesian National Institute of Aeronautics and Space (LAPAN)

vegetation index derived using an optical sensor such as Landsat (Nuarsa & Nishio, 2007; Parsa & Domiri, 2013; Domiri, 2017) and MODIS (Huang et al., 2010; Kham, 2012; Wijesingha et al., 2015; Parsa et al., 2017). However, rice plants are commonly planted during the wet season, and Stubenrauch et al. (2006) pointed out that tropical areas of Indonesia have year-round high-, mid- or low-level cloud cover (Stubenrauch et al., 2006). Hence, it is not possible to attain optimal use of an optical remote sensing satellite system that is affected by weather and cloud cover. However, it is possible to use a multispectral camera aboard a surveillance aircraft for rice plant monitoring (Broto et al., 2017). Yet this approach is not without its own challenges, including the difficulty associated with radiometric correction and the greater amount of time needed for extensive land monitoring (Kushardono et al., 2015). Satellite remote sensing technology with a SAR sensor shows promise for monitoring the earth surface since it is not affected by the weather.

The potential to use C-band SAR in identifying the rice plant growth phase has been demonstrated utilising radar backscatter value (σ^0) on several polarisations, such as VV polarisation (Ribbes & Le Toan, 1996), HH, VV and HH/VV polarisations (Lam-Dao et al., 2007), VV and VH polarisations (Raviz et al., 2016; Nguyen et al., 2016), and VH polarisation (Nguyen & Wagner, 2017; Son et al., 2017). In these studies, the radar backscatter values on the polarisations of VV, VH and HH were subject to multi-temporal variation owing to several factors. These included the scattering mechanism and object geometry, which means it can be used for rice plant growth phase identification and monitoring.

Rice plant growth commonly lasts for 3–4 months, from the vegetative through to the ripening phase, depending on the environment and variety (Yoshida, 1981). The rice plant growth phase can be classified as follows (Yoshida, 1981; Fageria, 2007):

1. Vegetative phase; characterised by increased tillering and plant height, as well as increasing leaf area. This stage lasts for approximately 60 days, depending on the variety.
2. Reproductive phase; identified by the formation of panicle, culm elongation and flowering. This stage is susceptible to temperature changes and has a duration of 30 days.
3. Ripening phase; characterised by spikelet filling and leaf senescence. The length of ripening ranges from about 30 days to longer in low-temperature areas.

The aim of this study is to identify the rice plant growth phase of the Ciherang variety by obtaining radar backscatter values (σ^0) for VV polarisation and VH polarisation. This study will find the best model for the rice plant growth phase determination. The Ciherang variety was selected since it is commonly planted by farmers in Indonesia (Badan Litbang Pertanian, 2012). Optimisation was performed in the development of the rice plant growth phase model where samples were taken spatially from a certain rice paddy block. The Normalised Difference Polarisation Index (NDPI) and several texture features, namely entropy, homogeneity and the mean of the Grey-Level Co-occurrence Matrix (GLCM), were included as samples for their ability to increase accuracy (Kushardono, 2012; Chulafak et al., 2017).

2 MATERIALS AND METHODOLOGY

2.1 Location and Data

The study area is located in Sukamandi District, Subang Regency,

which is one of Indonesia's granary areas (see Figure 2-1). The rice paddy at the site, which is owned by PT Sang Hyang Seri, is divided into several blocks. Each block has its own variety and planting schedule. In this study, seven blocks (Table 2-1) containing similar varieties were used in order to construct the rice plant growth phase model.

Figure 2-1: Study area in Sukamandi District.

Both VH and VV polarisations of Sentinel 1 C-Band SAR data were used in this study with a spatial resolution of 10 x 10 metres. The SAR data were acquired on 6 June 2016, 24 July 2016, 17 August 2016, 29 August 2016, 10 September 2016, 4 October 2016, 16 October 2016, and 28 October 2016. The SAR data were selected based on the date of planting, which was obtained from the field. In addition, the date of rice planting was used to calculate the age of the rice plants after planting.

Table 2-1: Rice planting realisation.

Rice paddy block code	Date of Planting
SBG-01 (B 19)	27 May 2016
SBG-02 (B 31)	10 July 2016
SBG-03 (L 10)	22 June 2016
SBG-04 (L 42)	3 June 2016
SBG-05 (LK 1)	30 May 2016
SBG-06 (S 21)	28 June 2016
SBG-07 (S 40)	20 July 2016

2.2 Methods

The research method is outlined in the flowchart shown in Figure 2-2. This study used Level 1 Ground Range Detected (GRD) SAR data with Interferometric Swath mode. Level 1 GRD data denote that the data have been projected using an ellipsoid earth modeling approach (ESA, 2013).

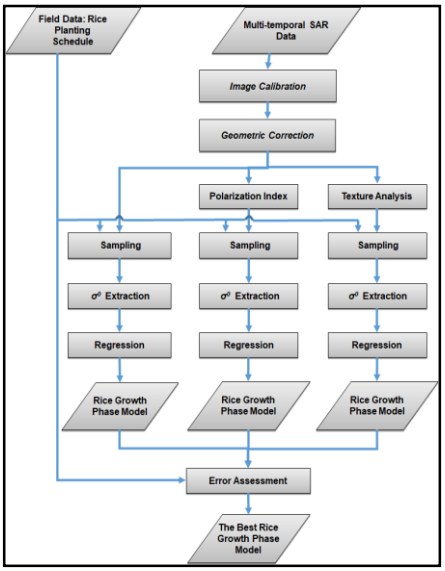

Figure 2-2: Research flowchart.

In the pre-processing stage, image calibration and geometric correction were performed on the Level 1 GRD SAR data. Image calibration was intended to remove the influence of incidence angle and signal power variation from the SAR data. Meanwhile, geometric correction was performed in order to reposition each pixel through geometrical operation (Choo et al., 2014).

Level 1 GRD SAR data consist of intensity and amplitude expressed in digital numbers. Conversion from the digital numbering to radar backscatter value (σ^0) was thus performed through image calibration according to the following equations (Grady et al., 2013; Miranda & Meadows, 2015).

$$\sigma^0_{dB} = 10.\log_{10}\sigma^0 \quad (2\text{-}1)$$

$$\sigma^0 = \frac{DN^2}{A^2_{dn}K}\sin(\alpha) \quad (2\text{-}2)$$

in which σ^0 is the radar backscatter value in decibels (dB), DN represents the digital number, α is the incidence angle, K is the calibration constant and A is the amplitude.

Samples were taken spatially from the rice paddy block in the pixel range of 80–100 in order to obtain representative samples for each phase of rice plant growth. This study employed three different criteria for samples. The first model was developed based on the single polarisation sample, namely VH and VV polarisation respectively (without the texture feature). The second model utilized the NDPI sample (without the texture feature). NDPI is expressed in the following equation (Kushardono, 2012).

$$\text{NDPI} = \frac{VH-VV}{VV+VH} \quad (2\text{-}3)$$

The last model was derived using the GLCM texture feature sample on VV and VH polarisation, such as entropy, homogeneity and GLCM mean (see Figure 2-2).

The sampling undertaken in each rice paddy block is shown in Figure 2-3. The radar backscatter values from the samples were extracted in order to obtain the rice plant growth phase models. The models were then tested using error assessment to acquire the best rice plant growth phase model.

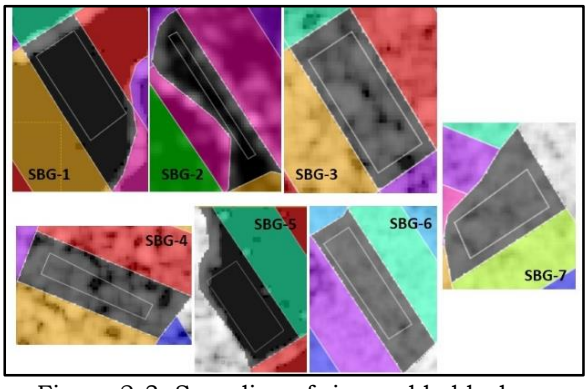

Figure 2-3: Sampling of rice paddy blocks.

Texture analysis based on spatial information of the radar backscatter values was performed using second-order GLCM statistics. Texture analysis is necessary inasmuch as high-resolution satellite images commonly contain important structure information and structure features capable of increasing accuracy (Kushardono et al., 1994; Zhang et al., 2017).

GLCM shows the probability (p) of the occurrence within an image of reference pixel with value i and neighboring pixel with value j, so that each element (i,j) is the number of occurrences between the reference pixel and neighboring pixel with value i and j (Pathak & Barooah, 2013). This study used the following texture analysis parameters:

1. Window size; window size can affect the amount of time taken for the data processing. The larger the window size, the more information is involved. This will lead to a reduction in the sharpness of the texture feature. However, a small window size will result in a rough texture feature. Accordingly, an optimal window size is needed. This study used a window size of 5x5 as this was able to give the most accurate result (Chulafak et al., 2017).
2. Quantisation; the grey-level quantisation used is 32. Quantisation affects the accuracy of texture analysis. However, the highest grey-level quantisation does not always lead to an increase in accuracy (Karthikeyan & Rengarajan, 2013).
3. Displacement; the displacement value used is 1 since a high displacement value can decrease accuracy and the optimal displacement values are 1 and 2 (Soh & Tsatsoulis, 1999).

4. Directional angle; all directional angles are used, giving a total of 8 directions.

Several texture features can be extracted from the texture analysis, namely contrast, homogeneity, entropy, dissimilarity, correlation, GLCM mean and variance (Haralick et al., 1973). Three of these, entropy, homogeneity and GLCM mean, were utilized as samples due to the high accuracy results (Chulafak et al., 2017).

3 RESULTS AND DISCUSSION

3.1 Without Texture Feature

Using the date of rice planting, the radar backscatter value of VH polarisation and VV polarisation were acquired at the rice plant ages after planting of 7 days, 10 days, 14 days, 26 days, 32 days, 40 days, 56 days, 68 days, 75 days, 87 days, 99 days, 104 days, 116 days and 128 days. The radar backscatter value on VH polarisation ranges from -24 to -15 dB, whereas the VV polarisation ranges from -14 to -8 dB. This occurs due to the depolarisation on the scattering mechanism of VH polarisation (Smith et al., 2012).

The variations in the VH polarisation and VV polarisation radar backscatter values with rice plant growth are depicted in Figures 3-1 a and b. The correlation between the two indicates a high correlation for VH polarisation where the square of the Pearson correlation coefficient, R^2, is 0.93 with a regression equation $y = 9.8 \ln (0.042\ln(x))$. Meanwhile, the correlation between the radar backscatter value of VV polarisation and rice plant growth is expressed in the regression equation of $y = -0.00000072x^4 + 0.00021x^3 - 0.02x^2 + 0.727x - 17.74$ with an R^2 of 0.55 and where x is the rice plant age after planting and y is the radar backscatter value.

The radar backscatter value is very low at the rice plant age of 7–14 days in Figure 3-1a. It indicates standing water that appears in the seedling stage. At this stage, the seeds are planted in flooded soil with a height of 3–5 cm. Under this condition, the radar signal applies in specular reflection such that the backscattered energy on VH polarisation is of a low intensity. This implies that the radar backscatter value is affected by surface roughness.

At the rice plant age of 26 days to 68 days, the radar backscatter value of VH polarisation steadily increases along with the increase of rice plant height and tillering number. A significant increase occurs at 68 days, which indicates the end of the vegetative phase and the beginning of the reproductive phase for the Ciherang variety. Therefore, the harvest season can be predicted by identifying the beginning of the reproductive phase. The rice plant growth phase model of VH polarisation in this study displays a similar trend to the results obtained by Raviz et al. (2016) and Nguyen et al. (2016).

The correlation coefficient value (R^2) of VV polarisation is relatively lower than for VH polarisation, which is probably due to the differences in the dominant scattering mechanism. It creates a strong soil moisture and leaf area index effect on VV polarisation, where the leaf area index can lead to attenuation of a return signal from the ground (Bousbih et al., 2017), meaning that the radar backscatter may fluctuate.

Figure 3-1b shows that the trend does not follow rice plant growth where there is a significant depression in the rice plant age between 40 and 87 days. This may occur as VV polarisation is strongly affected by the double-bounce scattering mechanism, soil moisture and the leaf area index (Nguyen et al., 2016; Bousbih et al., 2017). Soil moisture is influenced by water content, which has a high dielectric constant and results from

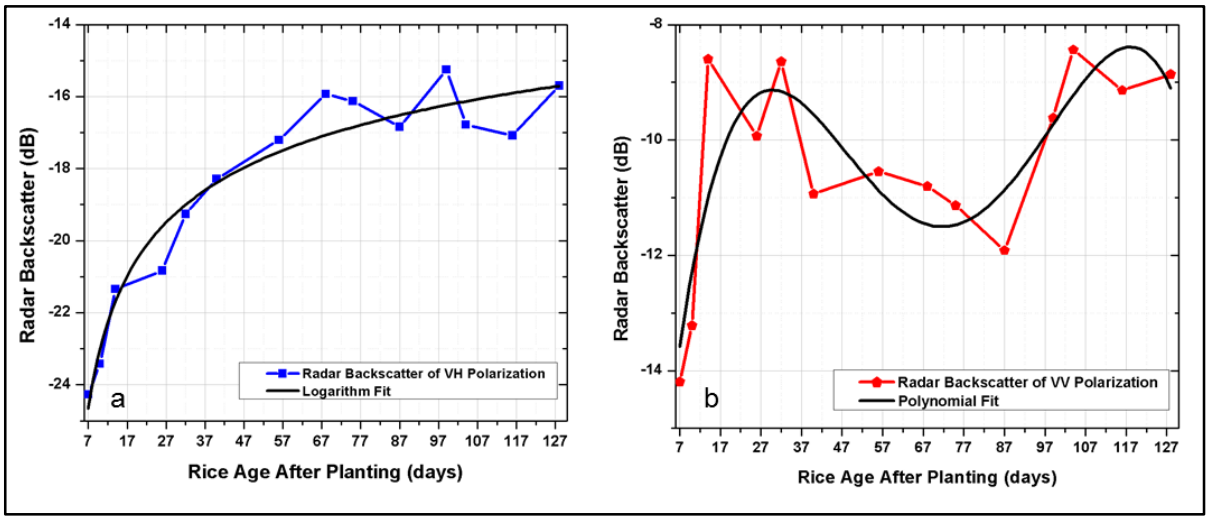

Figure 3-1: Relationship between rice plant growth and the radar backscatter value of (a) VH polarisation, (b) VV polarisation.

a rising radar backscatter value in the vegetative stage. Meanwhile, VH polarisation is comparatively not influenced by soil moisture inasmuch as its dominant scattering mechanism is volume scattering. The correlation between NDPI and rice plant growth is shown in Figure 3-2. It satisfies the regression equation of $y = -1.26E\text{-}11x^6 + 5.21E\text{-}9x^5 - 0.00000086x^4 + 0.000074x^3 - 0.00332x^2 + 0.067x - 0.08$, where x is the rice plant age after planting and y is NDPI with an R^2 of 0.67. The rice plant growth phase model from NDPI has a similar trend to the model generated from VV polarisation without texture feature, which shows there is a significant decrease in the radar backscatter value between the mid- vegetative phase and reproductive phase, although at a greater intensity compared
to VV polarisation. This depression in both models is similar to the trend in wheat identified by Fung and Ulaby (1983) and in rice as demonstrated by Nguyen et al. (2016).

Compared to the result in Nguyen et al., the rice variety observed from 10 m SAR data does not have a significant influence on radar backscatter value and the rice plant growth phase trend. It is seen by the radar backscatter value in this study, which is equivalent to that in Nguyen et al. (ranges from -23 to -15 dB for VH polarisation and from -16 to -7 dB for VV polarisation) [19].

3.2 With Entropy, Homogeneity and GLCM Mean Texture Feature

Figures 3-3a and b are variations of the radar backscatter value obtained by involving the entropy texture feature in both VH and VV polarisation. The correlation between the radar backscatter value of VH polarisation and rice plant growth is expressed by the logarithmic regression of $y = 7.65 \ln(0.32 \ln(x))$, where x is rice plant age after planting and y is the radar backscatter value with high correlation (R^2 =0.92). Furthermore, the correlation between the radar backscatter value of VV polarisation and rice plant growth satisfies the polynomial regression of $y = -0.00000047x^4 + 0.000137x^3 - 0.013x^2 + 0.446x + 3.30$ with an R^2 of 0.70. Involving the entropy texture feature, the rice plant growth phase model shows a resembling trend without texture feature's model. It implies that this model has the potential to be used in the identification and monitoring of the rice plant growth phase. Variations in the radar backscatter value involving the homogeneity texture feature on VH

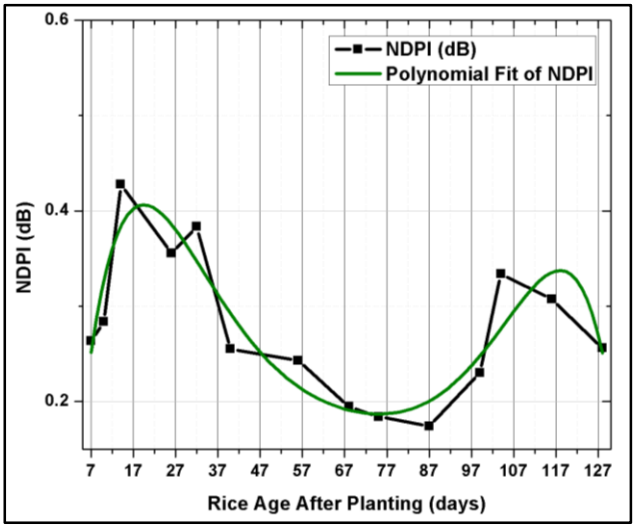

Figure 3-2: Relationship between NDPI and rice plant growth.

polarisation and VV polarisation are shown in Figures 3-3c and d. The correlation between the radar backscatter value on VH polarisation and rice plant growth is mathematically expressed by the regression equation of y = -1.56ln (0.074ln (x)) with an R^2 of 0.87. Meanwhile, the correlation between the radar backscatter value of VV polarisation and rice plant growth follows the polynomial regression of y = $0.00000073x^4$ $-0.0002x^3$ + $0.019x^2$ -0.62x +4.16, with an R^2 of 0.69. In those regressions, x represents the rice plant age after planting and y represents the radar backscatter value. The rice plant growth phase model involving the homogeneity texture feature trend shows an opposite trend to that of the rice plant growth phase model generated without the texture feature, entropy texture feature and GLCM mean texture feature on VH and VV polarisation. This model indicates that the homogeneity texture feature has a reciprocal relationship with the entropy texture feature, as seen on a graph in Gadkari (2004)

Figures 3-3 e and f depict variations of the radar backscatter value by involving the GLCM mean texture feature in VH and VV polarisation. The correlation between the radar backscatter value on VH polarisation and rice plant growth is represented by the regression equation y = 4.66 ln (0.89ln (x)) with an R^2 of 0.82. Then, the correlation between the radar backscatter value on VV polarisation and rice plant growth is obtained through the polynomial regression of y = $-0.000000101x^4$ + $0.000288x^3$ $-0.026x^2$ + 0.905x +3.51 with an R^2 of 0.63. The rice plant growth phase model with the GLCM mean texture feature exhibits a similar trend to that of the entropy texture features and without the texture feature on VH and VV polarisation, thus demonstrating its potential for use in the identification and monitoring of the rice plant growth phase.

3.3 Model Testing

The rice plant growth phase models obtained without texture feature, NDPI, and with texture features were evaluated using relative error assessment. Testing was performed using two samples from different rice paddy blocks. The samples were SBG-25/S 5 (Sample 1) and SBG-28/ S 8 (Sample 2) at the size of 80–100 pixels.

Figure 3-4 is the model testing result for VH polarisation and VV polarisation without texture feature. Based on the average error calculation, the smallest error for VH polarisation without texture feature is 4.98% (Sample

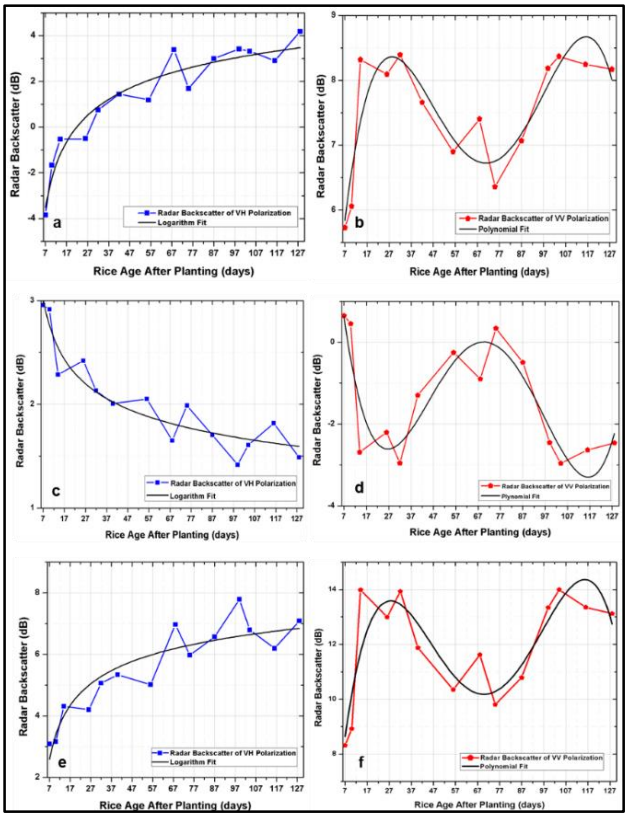

Figure 3-3: Relationship between radar backscatter value and rice plant growth for (a) entropy texture feature on VH polarisation, (b) entropy texture feature on VV polarisation, (c) homogeneity texture feature on VH polarisation, (d) homogeneity texture feature on VH polarisation, (e) GLCM mean texture feature on VH polarisation, (f) GLCM mean texture feature on VV polarisation.

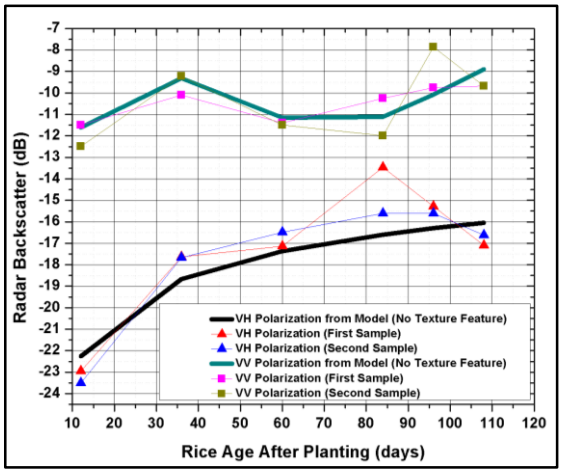

Figure 3-4: Testing result of rice plant growth phase model without texture feature.

2). Moreover, the smallest error for VV polarisation without texture feature is 5.20% (Sample 1). In general, both samples are reasonably fit with the model despite some inconsistency in the rice plant growth at 84 days on VH polarisation for Sample 1 and at 96 days on VV polarisation for Sample 2 due to depolarisation on the scattering mechanism. Figure 3-5 shows the model testing result of the NDPI rice plant growth phase model. The samples give average errors of 24.44% and 21.49% for Samples 1 and 2 respectively. Figures 3-6 and 3-7 show the model testing results of the rice plant growth phase model involving texture features, namely entropy, homogeneity and GLCM mean

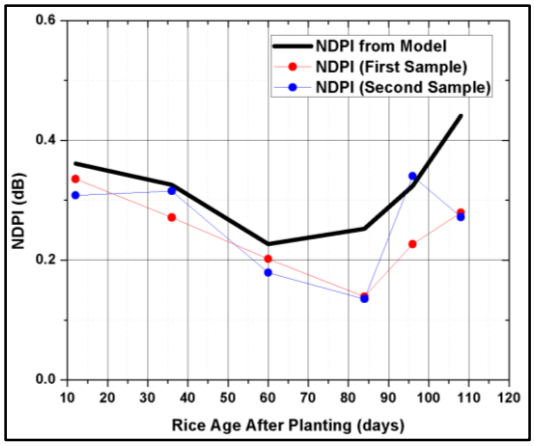

Figure 3-5: Testing result of rice plant growth phase model obtained from NDPI.

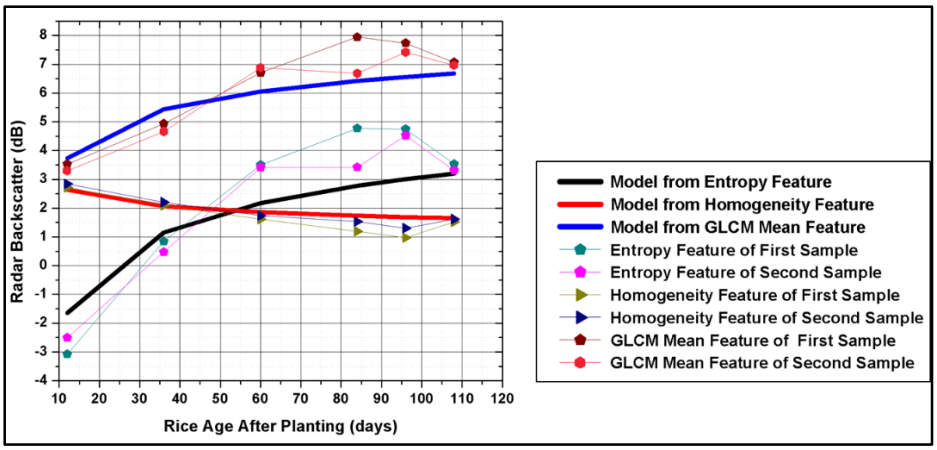

Figure 3-6: Testing result of rice plant growth phase model with texture feature on VH polarisation.

on VH polarisation and VV polarisation respectively. The smallest average error for Sample 1 on VH polarisation is 12.09% in the rice plant growth phase model with the GLCM mean texture feature and 9.47% for Sample 2 in the rice plant growth phase model with the homogeneity texture feature.

Furthermore, the smallest average error for Sample 1 on VV polarisation is 5.83% and for Sample 2 is 5.73% in the rice plant growth phase model with the entropy texture feature. The highest average error for VH polarisation is found in the rice plant growth phase models with the entropy texture feature, at 52.47% and 40.88% for Samples 1 and 2 respectively. Then, the highest average error for VV polarisation is in the rice plant growth phase models with the homogeneity texture feature, which are 75.17% and 71.41% for Samples 1 and 2 respectively. This finding is likely to have been influenced by the selection of the directional angle (all directions were used) when performing the texture analysis in this study, which can result in a loss of information on the diagonal matrix (Kushardono, 1996).

Table 3-1: Error assessment result on rice plant growth phase model

Sample Name	Average Error (%)								
	VH without Texture Feature	VV without Texture Feature	NDPI	VH with Entropy	VV with Entropy	VH with Homogeneity	VV with Homogeneity	VH with GLCM Mean	VV with GLCM Mean
Sample 1	6.94	5.20	24.44	52.47	5.83	16.49	75.17	12.09	6.35
Sample 2	4.98	8.38	21.49	40.88	5.73	9.47	71.41	10.14	9.91

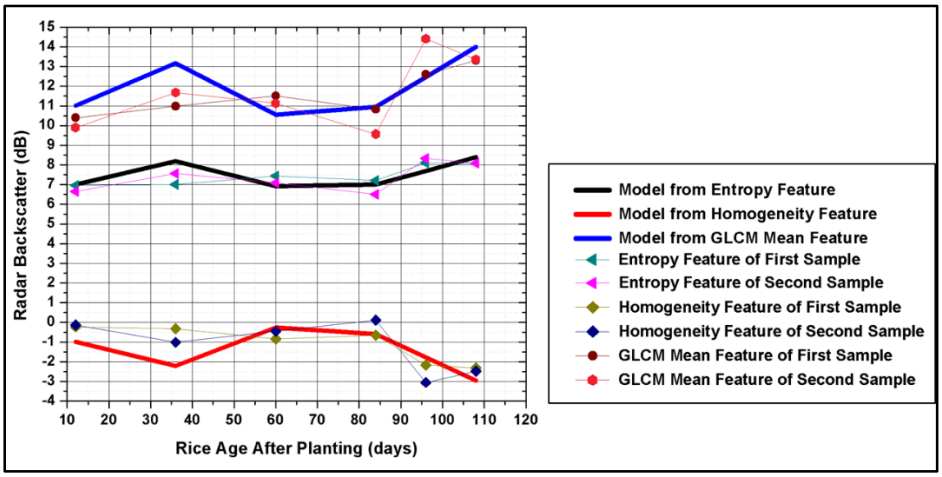

Figure 3-7: Testing result of rice plant growth phase model with texture feature on VV polarisation.

4 CONCLUSION

It can be concluded from this study that the radar backscatter value on VH polarisation can be used to identify the rice plant growth phase. The radar backscatter value of VH polarisation is relatively more sensitive to the rice plant growth phase than VV polarisation. The rice plant growth phase model from NDPI exhibits a similar trend to that of the rice plant growth phase model without texture feature on VV polarisation. The rice plant growth phase models on VH polarisation without texture feature, with entropy as well as the GLCM mean texture feature show a similar trend that may represent the rice plant growth phase up to the beginning of the reproductive phase. The rice plant growth phase models on VH polarisation without texture feature, with entropy and the GLCM mean texture feature show the potential to be developed for use in rice plant growth identification and monitoring. The rice plant growth phase model without texture feature on VH polarisation is shown to be the most suitable model since it produces the smallest average error.

ACKNOWLEDGEMENTS

The authors sincerely thank PT Sang Hyang Seri for providing the rice planting realisation data used in this research.

REFERENCES

Badan Litbang Pertanian (2012). Varietas Padi Unggulan *Maj. Agroinovasi Sinartani* 2–7.

Badan Pengkajian dan Pengembangan Perdagangan (2016). Potret Perdagangan Beras 1–2.

Badan Pusat Statistik Indonesia (2013). *Proyeksi Penduduk Indonesia (Indonesia Population Projection) 2010-2035*. Jakarta: Badan Pusat Statistik.

Bousbih, S., Zribi, M., Lili-Chabaane, Z., Baghdadi, N., El Hajj, M., Gao Q., & Mougenot, B. (2017). Potential of Sentinel-1 radar data for the assessment

of soil and cereal cover parameters, *Sensors (Switzerland)* 17, doi: 10.3390/s17112617

Broto, P. E., Saputro, A. H., & Kushardono, D. (2017). Prediction of paddy field area base on aerial photography using multispectral camera. *IEEE Conference on Sustainable Information Engineering and Technology (SIET), 1*, 425–9, doi: 10.1109/SIET.2017.8304176

Choo, A. L., Chan, Y. K., Koo, V. C., & Lim, T. S. (2014). Study on geometric correction algorithms for SAR images. *Int. J. Microw. Opt. Technol.,* 9, 68–72.

Chulafak, G. A., Kushardono, D., & Zylshal (2017). Optimasi parameter dalam klasifikasi spasial penutup penggunaan lahan menggunakan data Sentinel SAR. *J. Penginderaan Jauh,* 111–30, doi: 10.30536/j.pjpdcd.1017.v14.a2746

Domiri, D. D. (2017). The method for detecting biological parameter of rice growth and early planting of paddy crop by using multi temporal remote sensing data. *IOP Conf. Series: Earth and Environmental Science.*

ESA (2013). *Sentinel-1 User Handbook.*

Fageria, N. K. (2007). Yield physiology of rice. *J. Plant Nutr., 30*, 843–79, doi: 10.1080/15226510701374831

Ferencz, C., Bognár, P., Lichtenberger, J., Hamar, D., Tarcsai, G., Timár, G., Molnár, G., Pásztor, S., Steinbach, P., Székely, B., Ferencz, O. E., & Ferencz-Árkos, I. (2004). Crop yield estimation by satellite remote sensing. *Int. J. Remote Sens, 25*, 4113–49, doi: 10.1080/01431160410001698870

Fung, A. K., & Ulaby, F. T. (1983), *Manual of Remote Sensing* (Virginia: American Society of Photogrammetry).

Gadkari, D. (2004). *Image Quality Analysis Using GLCM.* Thesis, The University of Central Florida.

Grady, D. O., Leblanc, M., & Gillieson, D. (2013). Relationship of local incidence angle with satellite radar backscatter for different surface conditions, *Int. J. Appl. Earth Obs. Geoinf, 24*, 42–53, doi: 10.1016/j.jag.2013.02.005

Haralick, R. M., Shanmugam, K., & Dinstein, I. (1973). Textural features for image classification. *IEEE Trans. Syst. Man Cybern.* SMC 3, 610–21.

Huang, Q., Zhang, L., Wu, W., & Li, D. (2010) MODIS-NDVI-based crop growth monitoring in China Agriculture Remote Sensing Monitoring System. *Second ITA International Conference on Geoscience and Remote Sensing,* 287–90, doi: 10.1109/IITA-GRS.2010.5603948

Karthikeyan, S., & Rengarajan, N. (2013). Performance analysis of gray level cooccurrence matrix texture features for glaucoma diagnosis. *Am. J. Appl. Sci., 11*, 248–57, doi: 10.3844/ajassp.2014.248.257

Kham, D Van (2012). Using MODIS data for the monitoring growth and development of rice plants in Red River Delta, *VNU J. Sci. Earth Sci., 28*, 106–14.

Kushardono, D. (1996). *Study on High Accuracy Land Cover Classification Methods in Remote Sensing*. Disertation. Tokai University Research & Information Center

Kushardono, D. (2012). Klasifikasi spasial penutup lahan dengan data SAR dual-polarisasi menggunakan Normalised Difference Polarisation Index dan fitur keruangan dari matrik kookurensi. *J. Penginderaan Jauh*, 9, 12–24.

Kushardono, D., Anas, A., Maryanto, A., Utama, A. B., & Winanto (2015). Pemanfaatan data LSA (LAPAN Surveillance Aircraft) untuk mendukung pemetaan skala rinci. *Prosiding Pertemuan Ilmiah Tahunan XX MAPIN 2015,* doi: 10.13140/2.1.1504.3365

Kushardono, D., Fukue, K., Shimoda, H., & Sakata, T. (1994). Spatial land cover classification with the aid of neural network, *Proc. SPIE 2315 Image and Signal Processing for Remote Sensing* pp 702–10, doi: 10.1117/12.196770

Lam-Dao, N., Apan, A., Young, F., Le-Van, T.,

Le-Toan, T., & Bouvet, A. (2007). Rice monitoring using ENVISAT ASAR data: preliminary results of a case study in the Mekong River Delta, Vietnam. *Asian Conference on Remote Sensing* (Kuala Lumpur).

Mauludyani, A. V. R., Martianto, D., & Baliwati, Y. F. (2008). Pola konsumsi dan permintaan pangan pokok berdasarkan analisis data Susenas 2005. *J. Gizi dan Pangan, 3*, 101–17, doi: 10.25182/jgp.2008.3.2.101-117

Miranda, N., & Meadows, P. J. (2015). *Radiometric calibration of S-1 Level-1 Products generated by the S-1 IPF* (ESA).

Nguyen, D. B., Gruber, A., & Wagner, W. (2016). Mapping rice extent and cropping scheme in the Mekong Delta using Sentinel-1A data. *Remote Sens. Lett.,* 7, 1209–18, doi: 10.1080/2150704X.2016.1225172

Nguyen, D. B., & Wagner, W. (2017). European rice cropland mapping with Sentinel-1 data: The Mediterranean region case study. *Water (Switzerland), 9*, 1–21, doi: 10.3390/w9060392

Noor, M. (2015). Kebijakan pembangunan kependudukan dan bonus demografi. *Serat Acitya-Jurnal Ilm. UNTAG,* 121–8.

Nuarsa, I. W., & Nishio, F. (2007). Relationships between rice growth parameters and remote sensing data. *Int. J. Remote Sens. Earth Sci., 4*, pp102–12, doi: 10.30536/j.ijreses.2007.v4.a1221

Parsa, I. M., Dirgahayu, D., Manalu, J., Carolita, I., & Harsanugraha, K. W. (2017). Uji model fase pertumbuhan padi Berbasis citra MODIS multiwaktu di Pulau Lombok, *J. Penginderaan Jauh, 14*, 51–64.

Parsa, I. M., & Domiri, D. D. (2013). Multitemporal Landsat data to quick mapping of paddy field based on statistical parameters of vegetation index (case study : Tanggamus, Lampung), *Int. J. Remote Sens. Earth Sci., 10*, 19–24, doi: 10.30536/j.ijreses.2013.v10.a1838

Pathak, B., & Barooah, D. (2013). Texture analysis based on the gray-level co-occurrence matrix considering possible orientations. *Int. J. Adv. Res. Electr. Electron. Instrum. Eng.,* 2, 4206–12.

Raviz, J., Laborte, A., Barbieri, M., Mabalay, M. R., Garcia, C., Elena, J., Bibar, A., Mabalot P., & Gonzaga, H. (2016). Mapping and monitoring rice areas in Central Luzon, Philippines using X and C-band SAR imagery, *37th Asian Conference on Remote Sensing* (Colombo).

Ribbes, F., & Le Toan, T. (1996). Use of ERS-1 SAR data for ricefield mapping and rice crop parameters retrieval. *International Geoscience and Remote Sensing Symposium, 4*, 1983–5, doi: 10.1109/IGARSS.1996.516863

Soh, L., & Tsatsoulis, C. (1999). Texture analysis of SAR sea ice imagery using gray level co-occurrence matrices. *IEEE Transactions Geosci. Remote Sens., 37*, 780–95, doi: 10.1109/36.752194

Son, N., Chen, C-F., Chen, C-R., & Minh, V. (2017). Assessment of Sentinel-1A data for rice crop classification using random forests and support vector machines. *Geocarto Int., 33,* 587–601, doi: 10.1080/10106049.2017.1289555

Smith, R. B. (2012). *Introduction to interpreting digital radar images*. MicroImages, Inc.

Stubenrauch, C. J., Chédin, A., Rädel, G., Scott, N. A., & Serrar, S. (2006). Cloud properties and their seasonal diurnal variability from TOVS Path-B. *J. Clim., 19*, 5531–53, doi: 10.1175/JCLI3929.1

Yoshida, S. (1981). *Fundamentals of rice crop science*. Manila: International Rice Research Institute.

Wijesingha, J. S. J., Deshapriya, N. L., & Samarakoon, L. (2015). Rice crop monitoring and yield assessment with MODIS 250m gridded vegetation product: A case study in Sa Kaeo Province, Thailand. *36th International Symposium on Remote Sensing of Environment,* 40(Berlin), 121–7, doi: 10.5194/isprsarchives-XL-7-W3-121-2015

Zhang, X., Cui, J., Wang, W., & Lin, C. (2017).

A study for texture feature extraction of high-resolution satellite images based on a direction measure and gray level co-occurrence matrix fusion algorithm. *Sensors (Switzerland), 17*, doi: 10.3390/s17071474